

OccSora: 4D Occupancy Generation Models as World Simulators for Autonomous Driving

Lening Wang^{1,2,*†} Wenzhao Zheng^{2,3,*‡} Yilong Ren¹ Han Jiang¹

Zhiyong Cui¹ Haiyang Yu¹ Jiwen Lu³

<https://wzzheng.net/OccSora>

¹State Key Lab of Intelligent Transportation System, Beihang University, China

²EECS, UC Berkeley, United States ³Department of Automation, Tsinghua University, China

leningwang@buaa.edu.cn; wenzhao.zheng@outlook.com

Abstract

Understanding the evolution of 3D scenes is important for effective autonomous driving. While conventional methods model scene development with the motion of individual instances, world models emerge as a generative framework to describe the general scene dynamics. However, most existing methods adopt an autoregressive framework to perform next-token prediction, which suffer from inefficiency in modeling long-term temporal evolutions. To address this, we propose a diffusion-based 4D occupancy generation model, OccSora, to simulate the development of the 3D world for autonomous driving. We employ a 4D scene tokenizer to obtain compact discrete spatial-temporal representations for 4D occupancy input and achieve high-quality reconstruction for long-sequence occupancy videos. We then learn a diffusion transformer on the spatial-temporal representations and generate 4D occupancy conditioned on a trajectory prompt. We conduct extensive experiments on the widely used nuScenes dataset with Occ3D occupancy annotations. OccSora can generate 16s-videos with authentic 3D layout and temporal consistency, demonstrating its ability to understand the spatial and temporal distributions of driving scenes. With trajectory-aware 4D generation, OccSora has the potential to serve as a world simulator for the decision-making of autonomous driving. Code is available at: <https://github.com/wzzheng/OccSora>.

1 Introduction

As a promising application of artificial intelligence technology, autonomous driving has garnered widespread attention and research in recent years [16, 7, 46]. Establishing the relationship between perception [27, 3, 4, 29], prediction [14, 11, 24], and planning [32, 19, 20, 41] in autonomous driving is crucial for a comprehensive understanding of the field.

Conventional autonomous driving models [16] rely on the motion of the ego vehicle instances to model the development of scenes, unable to develop a profound understanding of scene perception and vehicle motion control comparable to human understanding. The emergence of world models [12] offers new possibilities for a deeper understanding of the comprehensive relationship between autonomous driving scenes and vehicle motion. Based on strong image pretrained models, image-based world models [15, 42] can generate high-quality driving-scene images with conditions of 3D bounding boxes. OccWorld [53] further learns a world model in the 3D occupancy space, which can be better leveraged for 3D reasoning for autonomous driving. However, most existing methods adopt an autoregressive framework to model the dynamics (e.g., image tokens, bounding boxes, occupancy) of a 3D scene, which hinders their ability to efficiently produce long-term video sequences.

*Equal contribution. †Work done during an internship at UC Berkeley. ‡Project leader.

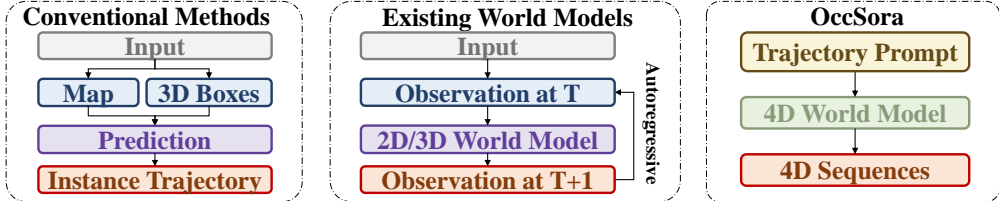


Figure 1: **Comparisons with existing methods.** It can comprehend the intricate relationship between scenes and trajectories and generate long-term, physically consistent 4D occupancy.

To address this, we propose a 4D world model OccSora to directly generate spatial-temporal representations with diffusion models as shown in Figure 1, motivated by OpenAI’s 2D video generation model Sora [1]. To accurately understand and represent 4D scenes, we design 4D scene discretization to capture the dynamic characteristics of scenes and propose a diffusion-based world model to achieve controllable scene generation following physical laws. Specifically, in the 4D occupancy scene tokenizer, we focus on extracting and compressing real 4D scenes to establish an understanding of the world model environment. In the diffusion-based world model, we employ multidimensional diffusion techniques to propagate accurate spatiotemporal 4D information and realize trajectory-controllable scene generation by incorporating real ego car trajectories as condition, thereby achieving a deeper understanding between autonomous driving scenes and vehicle motion control. Through training and testing, OccSora can generate autonomous driving 4D occupancy scenes that adhere to physical logic and achieve controllable scene generation based on different trajectories. The proposed autonomous driving 4D world model opens up new possibilities for understanding dynamic scene changes in autonomous driving and the physical world.

2 Related Work

3D Occupancy Prediction. 3D occupancy focuses on partitioning space into voxels and assigning specific semantic types to each voxel. It is considered a crucial means of representing real-world scenes, following 3D object detection [29, 28, 48] and Bird’s Eye View (BEV) perception [47, 52, 40, 51], for autonomous driving perception tasks. Early research on this task primarily focused on semantically classifying discrete points from LiDAR [55, 36, 25, 56]. In fact, due to the camera containing semantic information far exceeding that of LiDAR and their low cost. Thus, utilizing images for depth estimation or employing end-to-end methods for 3D scene perception research is currently the mainstream approach [18, 23, 44, 17]. Considering the advantages of multi-sensor systems, some studies research multi-modal fusion for 3D occupancy prediction [43, 49].

In addition to utilizing typical sensor devices for 3D occupancy prediction, some studies focus on other tasks involving occupancy. For instance, OccWorld [53] proposes a spatiotemporal generative transformer to predict subsequent scene tokens and the vehicle token, thereby predicting future occupancy and vehicle trajectory. On the other hand, GenOcc [39] utilizes generative models to accomplish occupancy prediction. DriveWorld [31] introduces a world-model-based framework for learning in autonomous driving from 2D images and videos, addressing tasks such as 3D object detection, online map creation, and occupancy prediction. Although progress has been made in 3D occupancy prediction and continuous 4D prediction, the scope of these studies remains limited. They usually use autoregressive models in conjunction with scene information from preceding frames to carry out subsequent occupancy tasks, thereby necessitating prior scene or 3D bounding box inputs. Consequently, they lack a genuine understanding of the fundamental relationships between scene and motion, and therefore do not constitute world models conditioned on actions.

Generative Model. Generative models have garnered widespread attention recently due to their powerful capabilities. By learning the probability distribution of data, generative models can train models capable of generating new samples. From the emergence of Generative Adversarial Networks (GAN) [10] to the recent advent of diffusion models like Variational Autoencoders (VAE) [37], the tasks of generative models have gradually expanded from initial image generation tasks to in-depth studies on videos [45]. Tasks such as image generation based on the DIT model [34] delve into and utilize their generative capabilities. The Sora video generation model [1] further demonstrates the ability to produce high-quality videos with realistic transitions between frames in continuous scenes.

Similarly, in the field of autonomous driving, controllable image generation can provide various driving scenarios to serve perception, planning, control, and decision-making tasks. For instance,

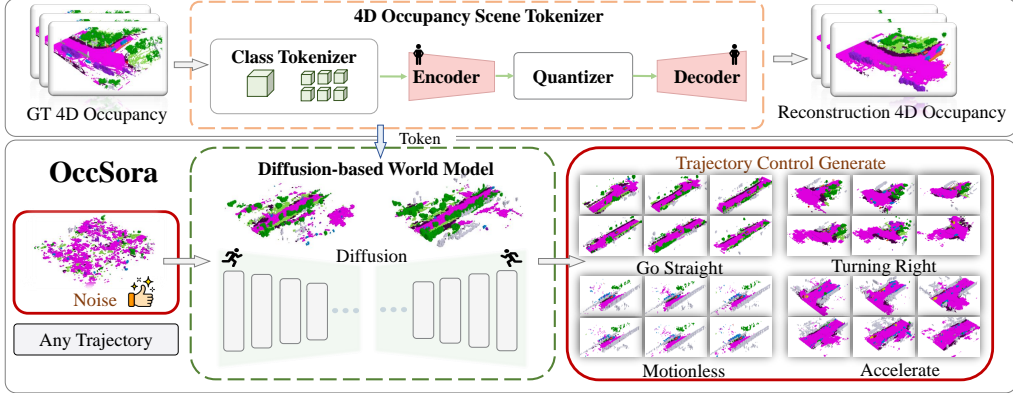


Figure 2: **The pipeline of OccSora.** The 4D occupancy scene tokenizer achieves compression and restoration of real information. The compressed information and vehicle trajectories are simultaneously used as inputs for the diffusion-based world model. After training, the diffusion-based world model utilizes random noise and arbitrary trajectories to generate controllable tokens, which are then decoded into 4D occupancy maps in the 4D occupancy scene tokenizer stage.

MagicDriver [8] generates videos depicting various weather scenarios by learning from videos of autonomous driving vehicles and incorporating labels such as object detection boxes and maps. DriveDreamer [42] proposes a world model that is entirely derived from real-world driving scenes, enabling a deep understanding of structured traffic constraints and thereby achieving precise and controllable video generation. However, for autonomous driving scenarios, obtaining the 3D occupancy of scenes is more important compared to 2D information [50, 30, 35]. Some studies [22, 26] propose a three-dimensional diffusion model suitable for generating outdoor real scenes, which, by utilizing diffusion methods, accomplishes scalable seamless scene generation tasks. While some previous studies have generated 2D static images and extended them to the temporal dimension through autoregression, and others have achieved static generation of 3D occupancy scenes, both the 2D images generated based on 3D object bounding boxes and the static large-scale scenes are difficult to directly apply to autonomous driving tasks [41, 54]. In contrast, our proposed OccSora establishes a dynamic 4D occupancy world model that adapts to scene changes with vehicle trajectories, without the need for any prior object detection boxes or scene information, representing the first generative 4D occupancy world model for autonomous driving.

3 Proposed Approach

3.1 World Model for Autonomous Driving

4D occupancy can comprehensively capture the structural, semantic, and temporal information of a 3D scene and effectively facilitate weak supervision or self-supervised learning, which can be applied to visual, LiDAR, or multimodal tasks. Based on these principles, we represent the world model χ as 4D occupancy R . Figure 2 illustrates the overall framework of OccSora. We constructed a 4D occupancy scene tokenizer to compress real 4D occupancy $R_{in} \in \mathbb{R}^{B \times D \times H \times W \times T}$ in both the temporal T and spatial $D \times H \times W$ dimensions, capturing the relationships and evolution patterns in 4D autonomous driving scenes. This results in compressed high-level tokens $R_{mi} \in \mathbb{R}^{B \times c \times h \times w \times t}$ and reconstructed 4D occupancy data $R_o \in \mathbb{R}^{B \times D \times H \times W \times T}$. We designed a diffusion-based world model that uses trajectory information $R_{tr} \in \mathbb{R}^{B \times T \times 2}$ as control units, training them supervised by the compressed tokens R_{mi} to generate high-dimensional scene representation tokens $T_o \in \mathbb{R}^{B \times c \times h \times w \times t}$. They are then decoded by the 4D occupancy scene tokenizer to consistent and dynamically controllable R_o .

3.2 4D Occupancy Scene Tokenizer

The goal of 4D occupancy prediction is to determine the semantic type at specific locations over time. We discretize and encode the real 4D occupancy scene R_{in} into an intermediate latent space R_{mi} to obtain a true representation of the 4D occupancy scene, as shown in Figure 3. The formula is as follows: $R_{mi} = \zeta_{token} \{ \tau_{en} (R_{in}) \}$. Here, ζ_{token} represents the encoded codebook, and τ_{en} denotes the designed 3D encoder network and category embedding. This 3D occupancy representation divides

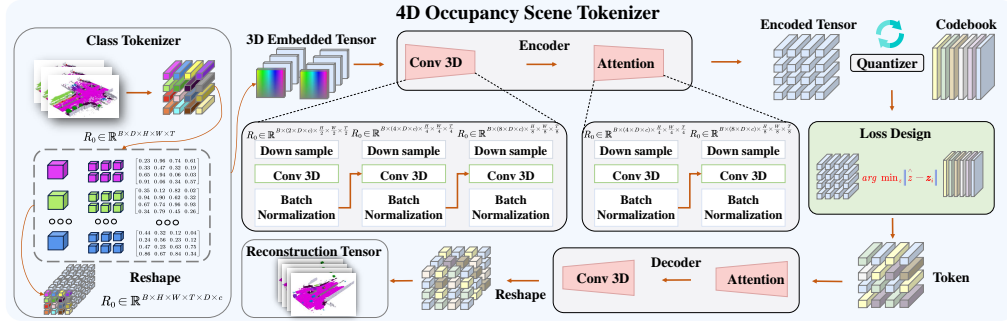


Figure 3: **The structure of the 4D occupancy scene tokenizer.** The proposed method encodes and compresses 4D scenes to extract high-dimensional features, which are then decoded to retrieve the spatiotemporal physical characteristics of the scenes.

the 3D space around the vehicle into voxels $r^T = N \in \mathbb{R}^{H \times W \times D}$, where each voxel position is assigned a type label N , indicating whether it is occupied and the semantics of the object occupying it. Unlike traditional methods, we incorporate and compress temporal information within the same scene, reshaping the tensor to R_{in} . This approach allows for unified learning of both spatial and temporal evolution patterns and the physical relationships of real scenes, compared to previous autoregressive methods. After passing through the τ_{en} 3D encoder network with category embedding and the ζ_{token} encoded codebook, the tensor is transformed into R_{mi} represents the potential spaces. This reshaping ensures a comprehensive representation of the temporal dynamics of 4D occupancy.

Category Embedding and Tokenizer. To accurately capture the spatial information of the original parameters, we first perform an embedding operation on the input R_{in} . We assign a learnable category embedding $b \in \mathbb{R}^{c'}$ for each category in R_{in} to label the categories of continuous 3D occupancy scenes. The position information is embedded as tokens that represent the categories. Then, these embeddings are concatenated along the feature dimension. To facilitate subsequent 3D encoding with compression in specific dimensions, we further reshape R_{in} into $R'_{in} \in \mathbb{R}^{B \times (Dc') \times T \times H \times W}$.

3D Video Encoder. To effectively learn discrete latent tokens, we further performed downsampling on the embedded positional information of the 4D occupancy R'_{in} to extract high-dimensional features. The designed encoder architecture comprises a series of 3D downsampling convolutional layers, which perform 3D downsampling in both the time dimension (T) and spatial dimensions (H \times W), increasing the fusion dimension to $D \times c'$. We initially downsampled the input R'_{in} three times to obtain $R''_{in} \in \mathbb{R}^{B \times (8 \times Dc') \times \frac{T}{8} \times \frac{H}{8} \times \frac{W}{8}}$, and introduced dropout layers after the feedforward and attention block layers for regularization. Considering the relationships between consecutive frames, we introduced cross-channel attention after downsampling, segmenting R''_{in} along the $8 \times Dc'$ dimension and then performing cross-channel attention between the segmented parts. This operation enhanced the model ability to capture relationships between features along different axes, and subsequently reshaped them back to the original shape to obtain the output tensor R_{mi} .

Codebook and Training Objective. To achieve a more condensed representation, we simultaneously learn a codebook $\zeta_{token} \in \mathbb{R}^{N \times D}$ containing N codes. Each code $b \in \mathbb{R}^{c'}$ in the codebook encodes a high-level concept of the scene, such as whether the corresponding position is occupied by a car.

ζ_{token} represents the encoded codebook. We quantize each spatial feature $\widehat{R}_{mi}^{(ij)}$ in \widehat{R}_{mi} by mapping it to the nearest code $N(\widehat{R}_{mi}^{(ij)}, B)$:

$$R_{mi}^{(ij)} = N(\widehat{R}_{mi}^{(ij)}, \zeta_{token}) = \min_{b \in \zeta_{token}} \|\widehat{R}_{mi}^{(ij)} - b\|_2, \quad (1)$$

where $\|\cdot\|_2$ represents the L2 norm. Subsequently, we integrate the quantized features $\widehat{R}_{mi}^{(ij)}$ to obtain the final scene representation R_{mi} .

3D Video Decoder. To reconstruct R_o from the learned scene representation R_{mi} , we design a decoder consisting of 3D deconvolution layers. In contrast to the encoder, the decoder architecture includes cross-channel attention, residual blocks, and a series of 3D convolutions, enabling upsampling in both temporal and spatial dimensions. This gradual upsampling process transforms R_{mi} to its original occupancy resolution R_o . The decoder then splits the result along the channel dimension

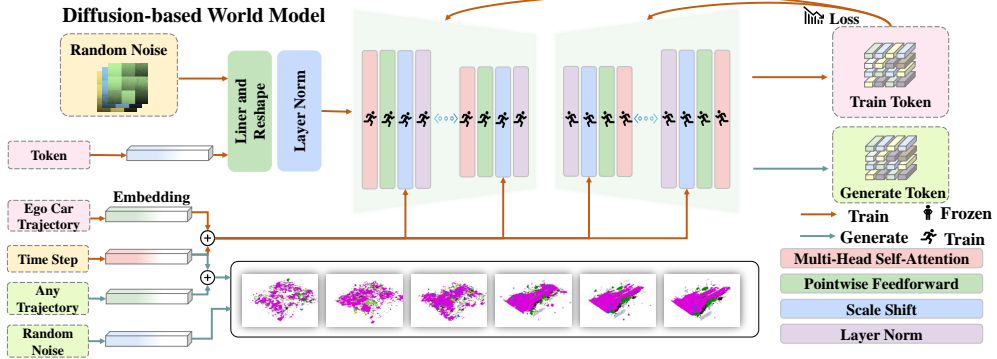


Figure 4: **The structure of the diffusion-based world model.** The model involves utilizing the optimal codebook obtained from training the 4D occupancy scene tokenizer to convert 4D occupancy into a sequence of tokens. These tokens, along with the ego vehicle trajectory and random noise, are then combined as input for denoising training to acquire the generated token.

to reconstruct the temporal dimension, yielding occupancy values for each voxel. During training, we accomplished the training of the encoder, decoder parameters, and the encoding codebook. The designed network enables us to simultaneously encode the input 4D occupancy information and compress it into multiple tokens, thereby learning the physical correlations of world models under spatiotemporal fusion. Additionally, we restore the information during the decoding process.

3.3 Diffusion-based World Model

Inspired by the diffusion method [33], we use scene tokens R_{mi} containing spatiotemporal information features as inputs for the generative model. Additionally, we conduct denoising training and trajectory-controllable generation tasks under the control of vehicle trajectories R_{tr} , as shown in Figure 4.

Token Embedding. To efficiently and accurately utilize the transformer [38], we flatten the input data tokens R_{mi} into R_{re} . Simultaneously, considering the significance of positional information for spatiotemporal compression, we perform positional embedding on the input. We design the following function, which utilizes sin and cos functions to encode positional indices:

$$R_{re}^{(emb)} = \text{emb}_i^d + R_{re}, R_{re} \in \mathbb{R}^{B \times c \times (hwt)}. \quad (2)$$

It operates on two main parameters: C , representing the embedding output dimensionality of each position, and $i = hwt$, representing the number of tokens enumerating the positions to be encoded. The resulting output follows a matrix structure of dimensions $C \times i$, and emb constructs the positional embedding representation using sin and cos functions. These embeddings encapsulate the positional attributes of the tokens, enhancing the model understanding of positions within the input. We add the positional encoding E_{mb} to the input R_{re} , yielding $R_{re}^{(emb)}$, which represents the tokens after positional encoding.

Trajectory Conditioning Embedding. The transformation relationship between scenes and trajectories is a crucial aspect of autonomous driving. Generating diverse 4D occupancy scenes that align with control trajectories is essential. Therefore, we use the ego vehicle trajectory T_r as input to generate controllable 4D occupancy. Firstly, the ego vehicle trajectory $T_r \in \mathbb{R}^{B \times t \times 2}$ is used as one of the control inputs, where t denotes the continuous time dimension, and the third dimension represents the vehicle positions along the x and y axes of the absolute coordinate system. To achieve trajectory embedding and encoding, we reshape the vehicle trajectory to $T_r \in \mathbb{R}^{B \times (t \times 2)}$ and learn and encode it as follows:

$$g = \nu(t) + \delta(T_r), \delta(T_r) \in \mathbb{R}^{B \times c \times (hwt)}, \nu \in \mathbb{R}^{B \times c \times (hwt)}, \quad (3)$$

where $\nu \in \mathbb{R}^{B \times c \times (hwt)}$ represents the time step embedding, and δ denotes the Multilayer Perceptron (MLP) network that extracts trajectory information. It is then embedded g into the input sequence of the diffusion transformer and processed together with the token information $R_{re}^{(emb)}$.

Diffusion Transformer. We developed a diffusion-based world model to learn from and generate within the latent space R_{mi} , while integrating trajectory labels T_r and denoising time steps ν as con-

trol conditions. In the model diffusion learning process, we constructed a forward noise process that gradually introduces noise to the latent space R_{mi} : $q(R_{re}^g|R_{re}) = N(R_{re}^g; \sqrt{\sigma^g}R_{re}, (1 - \sigma^g)I)$, where the constant g represents the embedding of trajectories and time steps. Utilizing the reparameterization trick, we can sample: $R_{re}^g = \sqrt{\sigma^g}R_{re} + \sqrt{1 - \sigma^g}\epsilon^g$, where $\epsilon^g \sim N(0, I)$. The 4D occupancy diffusion model is trained to learn the reverse propagation process. To invert the forward process corruption:

$$p_\theta(R_{re}^{g-1}|R_{re}^g) = N(\mu_\theta(R_{re}^g), \Sigma_\theta(R_{re}^g)), \quad (4)$$

where neural networks predict the statistical properties of p . The reverse process model is trained with the variational lower bound of x_0 , which simplifies to: $L(\theta) = -p(R_{re}^0|R_{re}^1) + \sum_g D_{KL}(q^*(R_{re}^{g-1}|R_{re}^g, R_{re}^0)) || p_\theta(R_{re}^{g-1}|R_{re}^g)$, which excluding irrelevant additional terms during training. As both q and p are gaussian distributions, the Kullback-Leibler (KL) divergence can be evaluated using the means and covariances of the two distributions. By reparameterizing as a noise prediction network, the model can be trained using the simple mean squared error between the predicted noise \hat{R}_{re}^g and the sampled gaussian noise R_{re}^g : $L_{simple}(\theta) = \frac{1}{2}(\hat{R}_{re}^g - R_{re}^g)^2$. However, to train the diffusion model with learned reverse process covariance, the full KL divergence term needs to be optimized. We follow diffusion models approach [6]: train first with $L_{simple}(\theta)$, then with the full L . Once p is trained, new token can be sampled by initializing $R_{re}^g \sim N(0, I)$ and sampling $R_{re}^{g-1} \sim p(R_{re}^{g-1}|R_{re}^g)$ using the reparameterization trick.

Overall, tokens R_{mi} processed in the initial stage as R_{re} are passed to a series of transformer blocks for further refinement. These blocks effectively capture the relationships between trajectory information and tokens. Regarding noisy image input processing, the diffusion transformer employs specific attention mechanisms and loss functions to minimize the impact of noise on model performance, ensuring robust operation in noisy environments. To incorporate trajectory labels T_r and denoising time steps ν as additional control conditions, we feed them as supplementary inputs alongside token embeddings into the transformer blocks. This enables the model to dynamically adjust its processing based on these conditions, thereby better adapting to various trajectory control requirements. In the end, the trained diffusion-based world model successfully transforms pure noise and trajectory labels T_r into $T_o \in \mathbb{R}^{B \times c \times h \times w \times t}$, which are eventually decoded into R_o through the 3D decoder.

4 Experiments

As a 4D occupancy world model in the field of autonomous driving, OccSora offers a deeper understanding of the relationship between autonomous driving scenes and vehicle trajectories without requiring any input of 3D bounding boxes, maps, or historical information. It can construct a long-time sequence world model that adheres to physical laws. We have conducted a series of quantitative experiments and visualizations to illustrate this.

4.1 Implementation Details

We conducted experiments on the widely used nuScenes-Occupancy dataset [2], which is currently one of the most mainstream and standard datasets, supporting many well-known research studies [16, 43]. For the OccSora model, we applied three rounds of compression to 32 consecutive frames and increased its channel dimension to 128. Subsequently, we conducted further comparative and ablation experiments under different components and trajectory scenarios. We trained using the AdamW optimizer with an initial learning rate set to 1×10^{-5} and a weight decay of 0.01. Using 8 NVIDIA GeForce A100 GPUs, we set a batch size of 2 per GPU. For the training of the 4D occupancy scene tokenizer, we needed about 42GB of memory per GPU to train for 150 epochs, which took 50.6 hours. For the diffusion-based world model, we needed about 47GB of memory per GPU to train for 1,200,000 steps, which took 108 hours.

4.2 4D Occupancy Reconstruction

The compression and reconstruction of 4D occupancy are essential for learning the latent spatiotemporal correlations and features necessary for image generation. Unlike traditional models for video and image processing, OccSora operates one dimension higher than occupancy for single frames

Table 1: **The quantitative analysis of 4D occupancy reconstruction.** Despite a compression rate 32 times greater than OccWorld, OccSora maintains over half of its reconstruction accuracy compared to OccWorld.

Method	Ratio	IoU	mIoU	Others	barrier	bicycle	bus	car	const. veh.	motorcycle	pedestrian	traffic cone	trailer	truck	drive. suf.	other flat	sidewalk	terrain	man made	vegetation
OccWorld [53]	16	62.2	65.7	45.0	72.2	69.6	68.2	69.4	44.4	47.0	74.8	67.6	54.1	65.4	48.2	77.8	46.9	76.6	45.2	84.3
OccSora	512	37.0	27.4	11.7	22.6	0.0	34.6	29.0	16.6	8.7	11.5	3.5	20.1	29.0	0.61	13.38	7.36	5.31	1.12	0.18

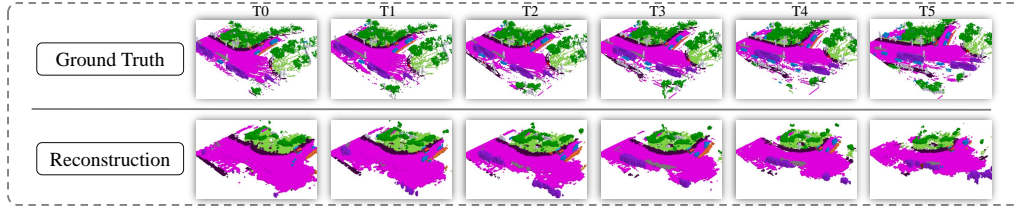


Figure 5: **Visualization of reconstruction of the 4D occupancy scene tokenizer.**

Table 2: **Comparisons of OccSora with other models in its generation capability.** To the best of our knowledge, we are the first 4D occupancy generation model. Therefore, we only provide comparisons with other generative models on different datasets and data formats.

Method	Type	Dimension	Dataset	FID
DiT [34]	Image	2D	ImageNet [5]	12.03
MagicDriver [8]	Video	3D	nuScenes [2]	14.46
DriveDreamer [42]	Video	3D	nuScenes [2]	14.9
DriveGAN [21]	Video	3D	nuScenes [2]	27.8
SemCity [22]	Occupancy	3D	KITTI [9]	40.63
OccSora	Occupancy Video	4D	nuScenes [2]	8.348

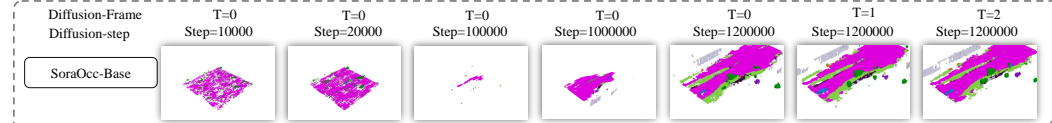


Figure 6: **The visualization of the progressive generation of accurate scenes as the model undergoes iterative training.**

and two dimensions higher than images. Therefore, achieving efficient compression and accurate reconstruction is paramount. Figure 5 depicts the ground truth and reconstruction of the occupancy. We also conducted a quantitative analysis of 4D occupancy reconstruction, as shown in Table 1. The table indicates that even with OccSora achieving a compression ratio 32 times greater than that of OccWorld, it still maintains nearly 50% mIoU of the original OccWorld model. This unified temporal compression effectively captures the dynamic changes of various elements, improving long-sequence modeling capabilities compared to progressive autoregressive methods.

4.3 4D Occupancy Generation

In the diffusion-based world model for the 4D occupancy generation task, we used tokens generated by the OccSora model, trained with 32 frames, as input for our generation experiments. In Figure 6, we present the visual results of across training iterations, from 10,000 to 1,200,000 steps. These visual results indicate that as the number of training iterations increases, the accuracy of the OccSora model continuously improves, demonstrating the generation of coherent scenes.

We compared and quantitatively evaluated our proposed OccSora model against other generation models. As the first 4D occupancy world model for autonomous driving, we only compared it against conventional image generation, 2D video generation, and static 3D occupancy scene generation methods. As shown in Table 2, our model achieves similar performance in terms of the Fréchet Inception Distance (FID) [13], demonstrating the effectiveness of the proposed method.

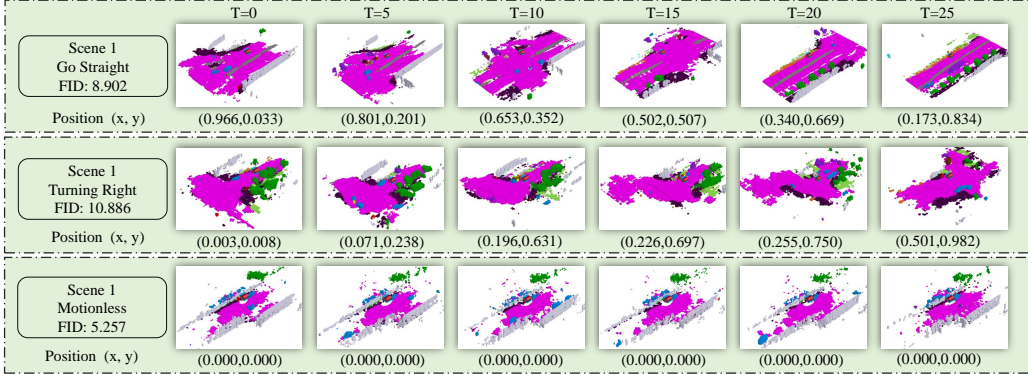


Figure 7: **4D occupancy generation under different input trajectories.** From top to bottom, there is go straight, turning right, and motionless, with each scene generation corresponding to the trajectory, ensuring logical coherence and continuity.

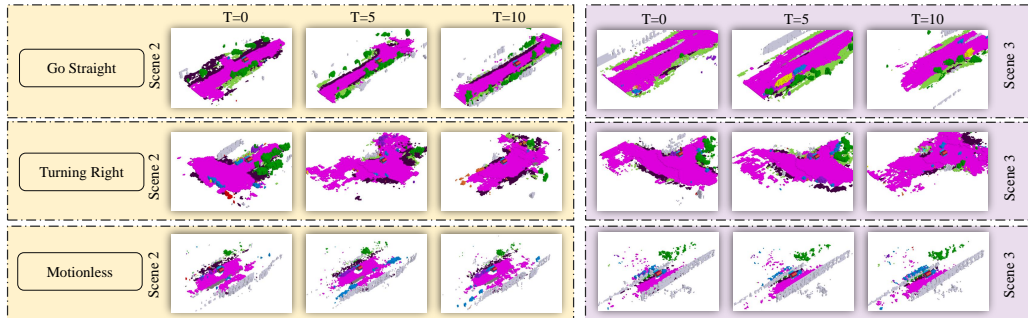


Figure 8: **Generating diverse continuous scenes under trajectory control.** The generated scenes exhibit diversity while maintaining the stability of the original trajectory control.

Table 3: **Results of ablative evaluation on different components.** We quantitatively evaluated the impact of different compression rates, components, and channel dimensions on the reconstruction and generation results through controlled variables.

Input Size R_{in}	Token Size R_{mi}	Channel	Class	T embed.	Trajectory	IoU	mIoU	FID
32x200x200	128x4x25x25	8	✓	✓	✓	37.03	27.42	8.34
32x200x200	128x4x25x25	8	✓	✗	✓	37.03	27.42	87.26
32x200x200	128x4x25x25	8	✓	✓	✗	37.03	27.42	17.48
32x200x200	128x4x25x25	4	✓	✓	✓	29.67	23.21	34.24
32x200x200	128x8x50x50	8	✓	✓	✓	32.91	24.4	72.32
12x200x200	64x3x50x50	8	✓	✓	✓	26.73	14.12	187.78
12x200x200	64x3x25x25	8	✓	✓	✓	22.42	9.27	270.23
12x200x200	32x3x25x25	8	✓	✓	✓	13.60	3.85	465.18

Trajectory Video Generation. OccSora has the capability to generate various dynamic scenes based on different input trajectories, thus learning the relationship between ego vehicle trajectories and scene evolution in autonomous driving. As shown in Figure 7, we input different vehicle trajectory motion patterns into the model, demonstrating the 4D occupancy for go straight, turning right, and motionless. We conducted experiments at different scales for generating trajectories, revealing that the FID score is lowest for stationary scenes and higher for curved scene, indicating the complexity of continuously modeling curved motion scenes and the simplicity of modeling stationary scenes.

Scene Video Generation. Diversity in scenes is crucial under reasonable trajectory control. We tested the reconstruction of 4D occupancy scenes for different scenarios under three trajectories to verify the generalization performance of generating scenes under controllable trajectories. In Figure 8, the left and right parts respectively demonstrate the capability to generate different scenes under the same trajectory. In the reconstructed scenes, surrounding trees and road environments exhibit random variations while still maintaining the logic of the original trajectory, showcasing the ability to maintain robustness in generating scenes corresponding to the original trajectory and its generalization across different scenarios.

Table 4: **The quantitative analysis of different scales regarding denoising steps and denoising rates.** Denoising steps have a relatively minor impact on the model, whereas denoising rates and model scales significantly affect the quality of the generated outputs.

Step	Input Size R_{in}	Token Size R_{mi}	FID					
			10%	30%	50%	70%	90%	100%
10	32x200x200	128x4x25x25	49863	34927	17630	339	42	9.1
100	32x200x200	128x4x25x25	53297	29521	19471	1084	72	10.08
1000	32x200x200	128x4x25x25	32171	10284	5924	591	17	8.94
10	12x200x200	64x3x50x50	71293	54625	5644	7416	742	431
100	12x200x200	64x3x50x50	81274	53431	45346	3161	456	446
1000	12x200x200	64x3x50x50	43631	33415	17431	4366	379	353

	10 %	30 %	50 %	70 %	90 %	100 %
Go Straight 1000 Step						
Go Straight 100 Step						
Motionless 100 Step						

Figure 9: **Effect of the denoising ratios under different trajectories or denoising steps.** Denoising steps and trajectories have minor impacts while denoising ratios have a significant effect.

4.4 Ablation and Analysis

Analysis of the Tokenizer and Embeddings. We conducted an ablation of the proposed components including different compression scales, the number of class tokenizer discretizations, time-step embeddings, and vehicle trajectory embeddings, as shown in Table 3. When the number of class tokenizer discretizations was reduced from 8 to 4, the reconstruction accuracy dropped by approximately 18%. The FID score also declined after removing the time-step embeddings. Without position embeddings, the generated scenes lacked motion control and displayed almost linear movement patterns influenced by the data distribution. Additionally, at lower compression ratios, although the reconstruction performance was better compared to higher compression ratios, the lack of higher-dimensional feature correlations prevented the generation of effective scenes.

Analysis of the Generation Steps. The total number of denoising steps and the denoising rate can affect the generation quality to some extent. As shown in Figure 9, as the denoising rate increases, the generated scenes become progressively clearer. According to the quantitative results in Table 4, increasing the total number of denoising steps can improve generation accuracy to a certain extent. However, the generation quality is much more significantly influenced by the token size and the number of channels than by the total number of denoising steps.

5 Conclusion and Limitations

In this paper, we have introduced a framework for generating 4D occupancy to simulate 3D world development in autonomous driving. Using a 4D scene tokenizer, we obtain compact representations for input and achieve high-quality reconstruction for long-sequence occupancy videos. Then, we learn a diffusion transformer on the spatiotemporal representations and generate 4D occupancy conditioned on a trajectory prompt. Through experiments on the nuScenes dataset, we demonstrate accurate scene evolution. In the future, we will investigate more refined 4D occupancy world models and explore the possibilities of end-to-end autonomous driving under closed-loop settings.

Limitations. The advantage of a 4D occupancy world model lies in establishing an understanding of the relationship between scenes and motion. However, due to limitations in the granularity of voxel data, we cannot construct more finely detailed 4D scenes. The generative results also demonstrate inconsistent details for moving objects, possibly due to the small size of the training data.

References

- [1] Tim Brooks, Bill Peebles, Connor Holmes, Will DePue, Yufei Guo, Li Jing, David Schnurr, Joe Taylor, Troy Luhman, Eric Luhman, Clarence Ng, Ricky Wang, and Aditya Ramesh. Video generation models as world simulators. 2024.
- [2] Holger Caesar, Varun Bankiti, Alex H Lang, Sourabh Vora, Venice Erin Liang, Qiang Xu, Anush Krishnan, Yu Pan, Giancarlo Baldan, and Oscar Beijbom. nuscenes: A multimodal dataset for autonomous driving. In *In CVPR*, pages 11621–11631, 2020.
- [3] Cheng Chang, Jiawei Zhang, Kunpeng Zhang, Wenqin Zhong, Xinyu Peng, Shen Li, and Li Li. Bevv2x: cooperative birds-eye-view fusion and grid occupancy prediction via v2x-based data sharing. *IEEE Transactions on Intelligent Vehicles*, 2023.
- [4] Xuanyao Chen, Tianyuan Zhang, Yue Wang, Yilun Wang, and Hang Zhao. Futr3d: A unified sensor fusion framework for 3d detection. In *In CVPR*, pages 172–181, 2023.
- [5] Jia Deng, Wei Dong, Richard Socher, Li-Jia Li, Kai Li, and Li Fei-Fei. Imagenet: A large-scale hierarchical image database. In *In CVPR*, pages 248–255. Ieee, 2009.
- [6] Prafulla Dhariwal and Alex Nichol. Diffusion models beat gans on image synthesis, 2021.
- [7] Daocheng Fu, Xin Li, Licheng Wen, Min Dou, Pinlong Cai, Botian Shi, and Yu Qiao. Drive like a human: Rethinking autonomous driving with large language models. In *In WACV*, pages 910–919, 2024.
- [8] Ruiyuan Gao, Kai Chen, Enze Xie, Lanqing Hong, Zhenguo Li, Dit-Yan Yeung, and Qiang Xu. Magicdrive: Street view generation with diverse 3d geometry control. *arXiv preprint arXiv:2310.02601*, 2023.
- [9] Andreas Geiger, Philip Lenz, and Raquel Urtasun. Are we ready for autonomous driving? the kitti vision benchmark suite. In *In CVPR*, pages 3354–3361. IEEE, 2012.
- [10] Ian Goodfellow, Jean Pouget-Abadie, Mehdi Mirza, Bing Xu, David Warde-Farley, Sherjil Ozair, Aaron Courville, and Yoshua Bengio. Generative adversarial networks. *Communications of the ACM*, 63(11):139–144, 2020.
- [11] Junru Gu, Chenxu Hu, Tianyuan Zhang, Xuanyao Chen, Yilun Wang, Yue Wang, and Hang Zhao. Vip3d: End-to-end visual trajectory prediction via 3d agent queries. *arXiv preprint arXiv:2208.01582*, 2022.
- [12] David Ha and Jürgen Schmidhuber. World models. 2018.
- [13] Martin Heusel, Hubert Ramsauer, Thomas Unterthiner, Bernhard Nessler, and Sepp Hochreiter. Gans trained by a two time-scale update rule converge to a local nash equilibrium, 2018.
- [14] Anthony Hu, Zak Murez, Nikhil Mohan, Sofía Dudas, Jeffrey Hawke, Vijay Badrinarayanan, Roberto Cipolla, and Alex Kendall. Fiery: Future instance prediction in bird’s-eye view from surround monocular cameras. In *ICCV*, 2021.
- [15] Anthony Hu, Lloyd Russell, Hudson Yeo, Zak Murez, George Fedoseev, Alex Kendall, Jamie Shotton, and Gianluca Corrado. Gaia-1: A generative world model for autonomous driving. *arXiv preprint arXiv:2309.17080*, 2023.
- [16] Yihan Hu, Jiazh Yang, Li Chen, Keyu Li, Chonghao Sima, Xizhou Zhu, Sici Chai, Senyao Du, Tianwei Lin, Wenhai Wang, et al. Planning-oriented autonomous driving. In *In CVPR*, pages 17853–17862, 2023.
- [17] Yuanhui Huang, Wenzhao Zheng, Borui Zhang, Jie Zhou, and Jiwen Lu. Selfocc: Self-supervised vision-based 3d occupancy prediction. *arXiv preprint arXiv:2311.12754*, 2023.
- [18] Yuanhui Huang, Wenzhao Zheng, Yunpeng Zhang, Jie Zhou, and Jiwen Lu. Tri-perspective view for vision-based 3d semantic occupancy prediction. In *In CVPR*, pages 9223–9232, 2023.
- [19] Zhiyu Huang, Haochen Liu, Jingda Wu, and Chen Lv. Differentiable integrated motion prediction and planning with learnable cost function for autonomous driving. *IEEE transactions on neural networks and learning systems*, 2023.
- [20] Xiaosong Jia, Penghao Wu, Li Chen, Jiangwei Xie, Conghui He, Junchi Yan, and Hongyang Li. Think twice before driving: Towards scalable decoders for end-to-end autonomous driving. In *In CVPR*, pages 21983–21994, 2023.
- [21] Seung Wook Kim, Jonah Philion, Antonio Torralba, and Sanja Fidler. Drivegan: Towards a controllable high-quality neural simulation. In *In CVPR*, pages 5820–5829, June 2021.
- [22] Jumin Lee, Sebin Lee, Changho Jo, Woobin Im, Juhyeong Seon, and Sung-Eui Yoon. Semicity: Semantic scene generation with triplane diffusion. *arXiv preprint arXiv:2403.07773*, 2024.
- [23] Yiming Li, Zhiding Yu, Christopher Choy, Chaowei Xiao, Jose M Alvarez, Sanja Fidler, Chen Feng, and Anima Anandkumar. Voxformer: Sparse voxel transformer for camera-based 3d semantic scene completion. In *In CVPR*, pages 9087–9098, 2023.

[24] Ming Liang, Bin Yang, Wenyuan Zeng, Yun Chen, Rui Hu, Sergio Casas, and Raquel Urtasun. Pnpnet: End-to-end perception and prediction with tracking in the loop. In *CVPR*, 2020.

[25] Xinhao Liu, Moonjun Gong, Qi Fang, Haoyu Xie, Yiming Li, Hang Zhao, and Chen Feng. Lidar-based 4d occupancy completion and forecasting. *arXiv preprint arXiv:2310.11239*, 2023.

[26] Yuheng Liu, Xinkle Li, Xuetong Li, Lu Qi, Chongshou Li, and Ming-Hsuan Yang. Pyramid diffusion for fine 3d large scene generation. *arXiv preprint arXiv:2311.12085*, 2023.

[27] Zhijian Liu, Haotian Tang, Alexander Amini, Xinyu Yang, Huizi Mao, Daniela L Rus, and Song Han. Bevfusion: Multi-task multi-sensor fusion with unified bird's-eye view representation. In *In ICRA*, pages 2774–2781. IEEE, 2023.

[28] Xinzhu Ma, Wanli Ouyang, Andrea Simonelli, and Elisa Ricci. 3d object detection from images for autonomous driving: a survey. *IEEE Transactions on Pattern Analysis and Machine Intelligence*, 2023.

[29] Jiageng Mao, Shaoshuai Shi, Xiaogang Wang, and Hongsheng Li. 3d object detection for autonomous driving: A comprehensive survey. *International Journal of Computer Vision*, 131(8):1909–1963, 2023.

[30] Lars Mescheder, Michael Oechsle, Michael Niemeyer, Sebastian Nowozin, and Andreas Geiger. Occupancy networks: Learning 3d reconstruction in function space. In *In CVPR*, pages 4460–4470, 2019.

[31] Chen Min, Dawei Zhao, Liang Xiao, Jian Zhao, Xinli Xu, Zheng Zhu, Lei Jin, Jianshu Li, Yulan Guo, Junliang Xing, et al. Driveworld: 4d pre-trained scene understanding via world models for autonomous driving. *arXiv preprint arXiv:2405.04390*, 2024.

[32] Sajjad Mozaffari, Omar Y Al-Jarrah, Mehrdad Dianati, Paul Jennings, and Alexandros Mouzakitis. Deep learning-based vehicle behavior prediction for autonomous driving applications: A review. *IEEE Transactions on Intelligent Transportation Systems*, 23(1):33–47, 2020.

[33] William Peebles and Saining Xie. Scalable diffusion models with transformers. *arXiv preprint arXiv:2212.09748*, 2022.

[34] William Peebles and Saining Xie. Scalable diffusion models with transformers. In *In ICCV*, pages 4195–4205, 2023.

[35] Chonghao Sima, Wenwen Tong, Tai Wang, Li Chen, Silei Wu, Hanming Deng, Yi Gu, Lewei Lu, Ping Luo, Dahua Lin, and Hongyang Li. Scene as occupancy. 2023.

[36] Gurpreet Singh, Soumyajit Gupta, Matthew Lease, and Clint Dawson. Range-net: A high precision streaming svd for big data applications. *arXiv preprint arXiv:2010.14226*, 2020.

[37] Aaron Van Den Oord, Oriol Vinyals, et al. Neural discrete representation learning. In *NeurIPS*, 30, 2017.

[38] Ashish Vaswani, Noam Shazeer, Niki Parmar, Jakob Uszkoreit, Llion Jones, Aidan N Gomez, Łukasz Kaiser, and Illia Polosukhin. Attention is all you need. In *NeurIPS*, 30, 2017.

[39] Guoqing Wang, Zhongdao Wang, Pin Tang, Jilai Zheng, Xiangxuan Ren, Bailan Feng, and Chao Ma. Occgen: Generative multi-modal 3d occupancy prediction for autonomous driving. *arXiv preprint arXiv:2404.15014*, 2024.

[40] Pengqin Wang, Meixin Zhu, Hongliang Lu, Hui Zhong, Xianda Chen, Shaojie Shen, Xuesong Wang, and Yinhai Wang. Bevgpt: Generative pre-trained large model for autonomous driving prediction, decision-making, and planning. *arXiv preprint arXiv:2310.10357*, 2023.

[41] Tianqi Wang, Sukmin Kim, Ji Wenxuan, Enze Xie, Chongjian Ge, Junsong Chen, Zhenguo Li, and Ping Luo. Deepaccident: A motion and accident prediction benchmark for v2x autonomous driving. In *In AAAI*, volume 38, pages 5599–5606, 2024.

[42] Xiaofeng Wang, Zheng Zhu, Guan Huang, Xinze Chen, and Jiwen Lu. Drivedreamer: Towards real-world-driven world models for autonomous driving. *arXiv preprint arXiv:2309.09777*, 2023.

[43] Xiaofeng Wang, Zheng Zhu, Wenbo Xu, Yunpeng Zhang, Yi Wei, Xu Chi, Yun Ye, Dalong Du, Jiwen Lu, and Xingang Wang. Openoccupancy: A large scale benchmark for surrounding semantic occupancy perception. In *In ICCV*, pages 17850–17859, 2023.

[44] Yi Wei, Linqing Zhao, Wenzhao Zheng, Zheng Zhu, Jie Zhou, and Jiwen Lu. Surroundocc: Multi-camera 3d occupancy prediction for autonomous driving. In *In ICCV*, pages 21729–21740, 2023.

[45] Wilson Yan, Yunzhi Zhang, Pieter Abbeel, and Aravind Srinivas. Videogpt: Video generation using vq-vae and transformers, 2021.

[46] Chenyu Yang, Yuntao Chen, Hao Tian, Chenxin Tao, Xizhou Zhu, Zhaoxiang Zhang, Gao Huang, Hongyang Li, Yu Qiao, Lewei Lu, et al. Bevformer v2: Adapting modern image backbones to bird's-eye-view recognition via perspective supervision. In *In CVPR*, pages 17830–17839, 2023.

[47] Lei Yang, Kaicheng Yu, Tao Tang, Jun Li, Kun Yuan, Li Wang, Xinyu Zhang, and Peng Chen. Bevheight: A robust framework for vision-based roadside 3d object detection. In *In CVPR*, pages 21611–21620, 2023.

- [48] Haibao Yu, Yingjuan Tang, Enze Xie, Jilei Mao, Ping Luo, and Zaiqing Nie. Flow-based feature fusion for vehicle-infrastructure cooperative 3d object detection. *In NeurIPS*, 36, 2024.
- [49] Ji Zhang and Yiran Ding. Occfusion: Depth estimation free multi-sensor fusion for 3d occupancy prediction. *arXiv preprint arXiv:2403.05329*, 2024.
- [50] Yunpeng Zhang, Zheng Zhu, and Dalong Du. Occformer: Dual-path transformer for vision-based 3d semantic occupancy prediction. In *In ICCV*, pages 9433–9443, 2023.
- [51] Yunpeng Zhang, Zheng Zhu, Wenzhao Zheng, Junjie Huang, Guan Huang, Jie Zhou, and Jiwen Lu. Beverse: Unified perception and prediction in birds-eye-view for vision-centric autonomous driving, 2022.
- [52] Yuan Zhao, Lu Zhang, Jiajun Deng, and Yanyong Zhang. Bev-radar: bidirectional radar-camera fusion for 3d object detection. *JUSTC*, 54(1):0101–1, 2024.
- [53] Wenzhao Zheng, Weiliang Chen, Yuanhui Huang, Borui Zhang, Yueqi Duan, and Jiwen Lu. Occworld: Learning a 3d occupancy world model for autonomous driving. *arXiv preprint arXiv:2311.16038*, 2023.
- [54] Wenzhao Zheng, Ruiqi Song, Xianda Guo, and Long Chen. Genad: Generative end-to-end autonomous driving. *arXiv preprint arXiv:2402.11502*, 2024.
- [55] Zixiang Zhou, Yang Zhang, and Hassan Foroosh. Panoptic-polarinet: Proposal-free lidar point cloud panoptic segmentation. In *In CVPR*, pages 13194–13203, 2021.
- [56] Sicheng Zuo, Wenzhao Zheng, Yuanhui Huang, Jie Zhou, and Jiwen Lu. Pointocc: Cylindrical tri-perspective view for point-based 3d semantic occupancy prediction. *arXiv preprint arXiv:2308.16896*, 2023.

A Appendix

A.1 More Visualizations

To provide results for longer time series, we present the generated scenes under different ego vehicle trajectory controls, namely Go Straight, Turning Right, Motionless, and Accelerate in Figure 10. Additionally, we also showcase the equivalent control methods under different scenes in Figure 11.

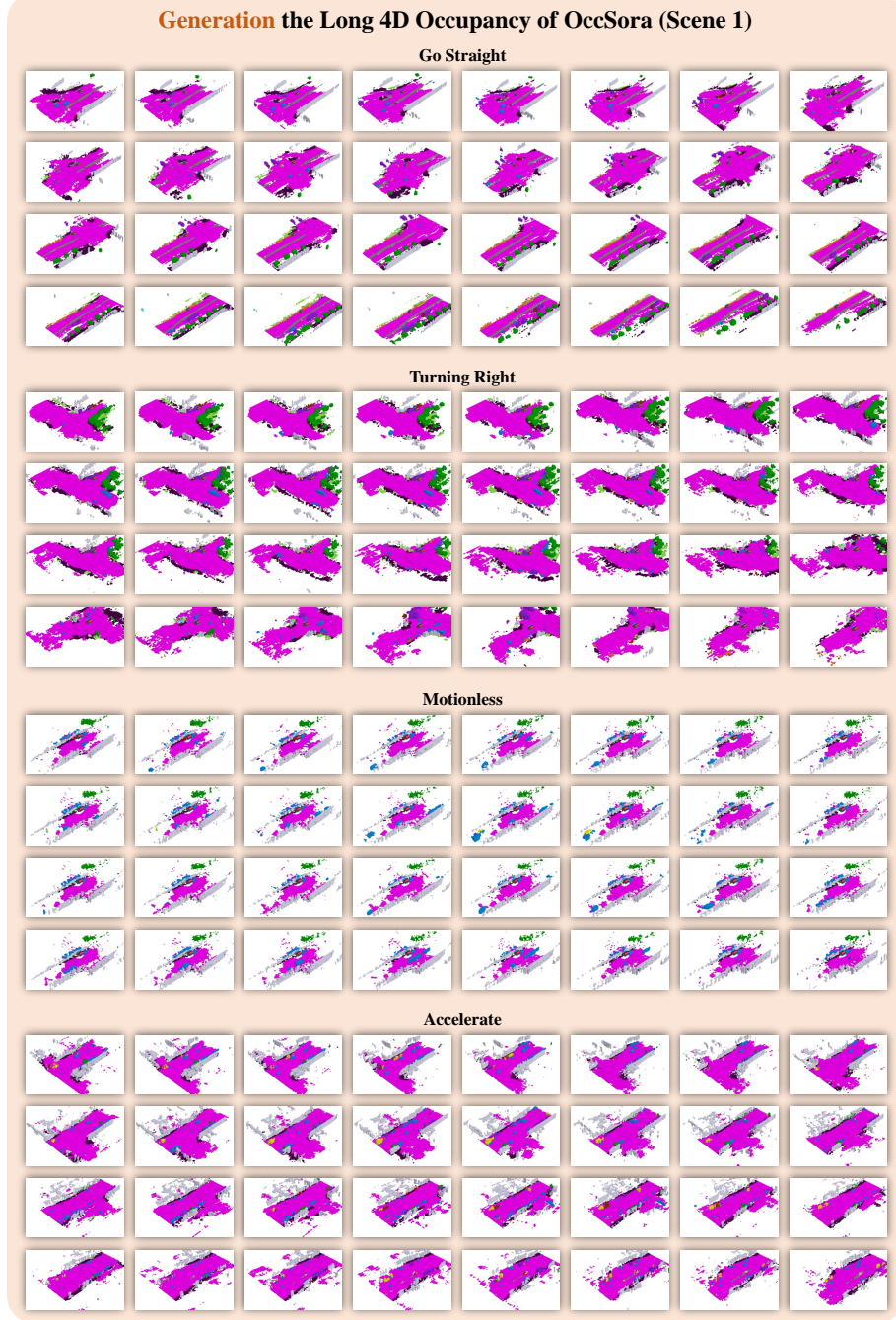


Figure 10: **The ability to generate long time-series 4D occupancy under different trajectory controls.** From top to bottom, we present long-term continuous scenes generated under four types of ego vehicle trajectories: Go Straight, Turning Right, Motionless, and Accelerate.

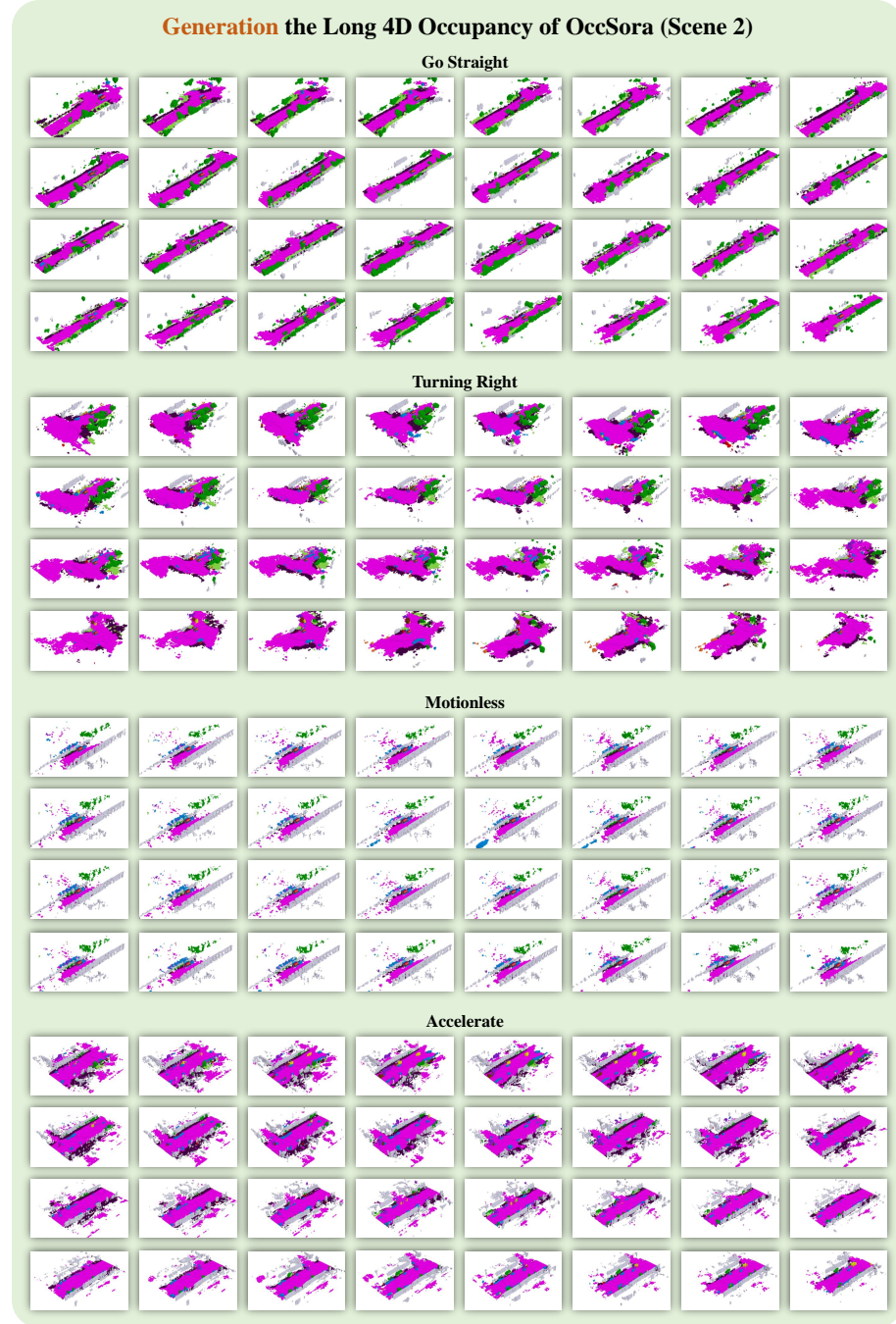


Figure 11: **The generalization ability to generate different scenes under fixed ego vehicle trajectories.** From top to bottom, we show the capabilities of generating different scenes under the four vehicle trajectories: Go Straight, Turning Right, Motionless, and Accelerate.